Organization of an Amphiphilic Graft Copolymer at the Air−Water Interface: A Neutron Reflectometry Study

S. K. Peace, R. W. Richards,* and M. R. Taylor

Interdisciplinary Research Centre in Polymer Science and Technology, University of Durham, Durham DH1 3LE, U.K.

J. R. P. Webster

ISIS Science Division, Rutherford Appleton Laboratory, Chilton Didcot, Oxon OX11 0QZ, U.K.

N. Williams

ICI Paints, Wexham Road, Slough SL2 5DS, U.K.

Received March 18, 1997; Revised Manuscript Received August 12, 1997

ABSTRACT: Graft copolymers of methyl methacrylate and ethylene oxide have been prepared with a methacrylate backbone and poly(ethylene oxide) grafts of 54 ethylene oxide units. Three copolymers with different ethylene oxide contents have been synthesized together with equivalent copolymers with deuteriomethyl methacrylate backbones. Each of these copolymers has been spread at the air−water interface and their organization investigated using neutron reflectometry. The reflectivity data have been analyzed using exact optical matrix and approximate partial structure factor methods. As the surface concentration and ethylene oxide content increases, the number of layers needed to reproduce the reflectivity data increases. The poly(ethylene oxide) grafts stretch deeper into the subphase as their areal density increases, and ideas from grafted brush layer theory have been applied to these data. Exact agreement is not obtained, and reasons for this have been cited. When the ethylene oxide content in the near surface layer is high, the partial structure factor of the water exhibits anomalous behavior.

Introduction

The behavior of polymers at fluid interfaces is important in a number of situations, antifoaming properties and emulsion stabilization being two examples. A crucial factor in determining the mechanical properties of the interfacial region and the response to perturbations is the organization of the polymer at the interface. Such interfaces are continually perturbed by stochastic thermal fluctuations that are collectively called the capillary waves;[1,2] the properties of the capillary waves are severely influenced by the presence of an interfacial layer[3] and in their turn these properties are germane to such aspects as flow instabilities and jet break up in fluid streams.[4]

Information on the organization of polymers at fluid interfaces is somewhat sparse due, in part, to the difficulty in obtaining data that provide the necessary insight. Ellipsometry,[5−7] ATR FTIR,[8,9] and X-ray reflectivity[10,11] have all been used on various polymer systems but detailed information about the organization of polymers at fluid interfaces is not really forthcoming from such techniques. In principle, X-ray reflectivity can give a detailed description of the interfacial organization because the spatial resolution is high. Unfortunately, the contrast generated by the difference in electron density between the constituents of the interfacial region is generally insufficiently large to be useful, except where heavy atoms are present. The reflectivity of neutrons from the interface on the other hand can provide all the required information when full advantage of deuterium labeling is taken to generate sufficient contrast between the species. Even when it is not possible to deuterate each component in the polymer, changing the deuterium content of the subphase can sometimes provide sufficient contrast to give additional insight.

Apart from correlating the organization of a polymer at an interface with such facets as the behavior of capillary waves, polymers at fluid interfaces constitute models for polymeric brush layers. Predictions concerning the thickness of brush layers and their dependence on the areal density of the polymer have been available since 1980.[12−14] Attempts at evaluating the veracity of such predictions were first made by using small-angle neutron scattering[15−17] and subsequently force−distance data for polymer-coated surfaces in a surface force balance.[18−22] Neutron reflectometry has been used to examine brushlike layers of polymers in the melt grafted to solid substrates and has been successful.[23−25] For polymers at fluid interfaces, use of neutron reflectometry to investigate the properties of brushlike layers has only been successful in one system where the subphase was an organic liquid and of low surface tension.[26] A direct attempt at using neutron reflectometry to observe brushlike layers was that of Field et al.[27] When the subphase is water, the surface tension is generally so high that any polymer that is solvated is adsorbed at the surface in a relatively thin layer compared to the dimensions of real brushlike layers. This is especially true where the solvated polymer is poly(ethylene oxide).

Neutron reflectometry has been applied to surface excess layers and spread films of this polymer.[28,29] Although differences in the nature of the surface films were evident, the region occupied by the poly(ethylene oxide) was ca. 30 Å thick at most. Linear block copolymers of poly(methyl methacrylate) (MMA) and poly(ethylene oxide) (EO) spread at the air−water interface

* To whom correspondence should be addressed.

S0024-9297(97)00363-X CCC: $15.00
Published on Web 01/30/1998

have also been studied.[30,31] In this case the two blocks are mixed at low surface concentrations but occupy different spatial regions at higher surface concentrations with the EO block being immersed in the subphase.

We discuss here the organization of *graft* copolymers with an MMA backbone and EO grafts that have been spread at the air−water interface. The EO content of the copolymers has been varied over a finite range and the change in interfacial organization investigated for discrete surface concentrations. Graft copolymers at fluid interfaces are of technological interest because for a given mass of polymer it may be possible to obtain a larger amount of the grafts in one of the fluid phases than by using a simple block copolymer. Additionally, the observation of brush behavior depends on having a high grafting density of the interface. Graft copolymers may approach the critical grafting density at lower total surface concentrations than the diblock copolymers or end-functionalized copolymers that have been used hitherto. Our aims were 2-fold: (i) to gain some insight into the influence of polymer architecture on the organization of an amphiphilic copolymer at the air−water interface and (ii) to investigate the applicability of a limited form of the kinematic approximation to neutron reflectivity data.

Neutron Reflectivity Theory

Full descriptions of the theory of neutron reflectometry are available in the literature,[32−34] we summarize the salient points here. When a beam of neutrons is incident on a plane surface at a glancing angle θ, some of the beam is specularly reflected and some is transmitted. The intensity of the specularly reflected beam is determined by the neutron refractive index, n, of the substance on which the beam is incident. If n varies with distance below the surface, then the transmitted beam will also be reflected to an extent depending on the value of n at the particular depth. All of the reflected beams incident on the detector will interfere in some way and the variation of the specularly reflected intensity with incident angle (usually expressed as momentum transfer, $Q = (4\pi/\lambda) \sin \theta$, λ is the neutron beam wavelength) will be characteristic of the variation in n normal to the surface. Ignoring any absorption effects, which are generally negligible for neutron reflectivity, then

$$n = 1 - \frac{\lambda^2}{2\pi}\rho \tag{1}$$

where ρ is the scattering length density and

$$\rho = \sum \frac{b_i m N_A}{d} \tag{2}$$

where b_i is the coherent scattering length of each atom, i, present in the material that has a molecular weight m and physical density d. If, at some point below the surface, there are several species, j, present each at a particular volume fraction, then the scattering length density at that depth, z, is

$$\rho(z) = \sum_j \phi_j \rho_j \tag{3}$$

Reflectivities can be calculated exactly using the optical matrix formalism if the near surface depth profile can be described by a series of lamellae of known thickness and scattering length density.

Analysis of reflectivity data is generally made by assuming a model for the variation in composition normal to the surface, calculating the values of ρ and hence reflectivity from this model. The reflectivity obtained is compared to the experimental value and the parameters of the model adjusted until acceptable agreement is obtained.

When the reflectivity is low ($<10^{-2}$) the kinematic approximation can be used and the reflectivity expressed using partial structure factors.[32,33] For the graft copolymer spread on water being discussed here there are three components, the MMA backbone, the EO grafts, and water. In the kinematic approximation the reflectivity from such a system is expressed as

$$R(Q) = \frac{16\pi^2}{Q^2}[b_m{}^2 h_{mm}(Q) + b_e{}^2 h_{ee}(Q) + b_s{}^2 h_{ss}(Q) + 2b_m b_e h_{me}(Q) + 2b_m b_s h_{ms}(Q) + 2b_e b_s h_{es}(Q)] \tag{4}$$

Where subscripts m, e, and s refer to methyl methacrylate, ethylene oxide, and subphase, respectively. The self-partial structure factors, $h_{ii}(Q)$, are the squares of the one-dimensional Fourier transforms of the number density distribution of species i normal to the surface. Analytical expressions can be written for these self-partial structure factors when relatively simple models are used to describe the neutron refractive index variation with depth. The self-partial structure factors contain the dimensions and compositions of the regions occupied by each species i. Cross-partial structure factors, $h_{ij}(Q)$, contain information about the separation of the regions from one another. When all partial structure factors are known, a detailed description of the surface organization becomes available, but obtaining these partial structure factors requires six simultaneous equations of the form of eq 4 to be solved. Under certain conditions, eq 4 can be simplified and we make use of the simpler forms of these equations later.

Experimental Section

Graft Copolymer Synthesis. Methoxy poly(ethylene glycol) methacrylate (MPEG) macromer (**1**) was supplied as a solution in a mixture of propylene glycol and water.

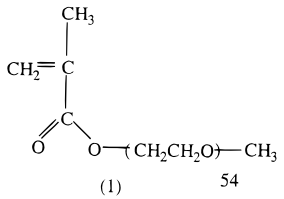

(1) 54

This solution was first rotary evaporated to remove water and then cooled to 273 K where the MPEG precipitated out. After MPEG was washed with ethanol at 273 K and drying under vacuum at 313 K, the ^{1}H NMR spectrum in $CDCl_3$ was obtained. Analysis of this spectrum indicated that the number of ethylene oxide segments per monomer unit was 54 ± 2. Methyl methacrylate (MMA) (hydrogenous and deutero forms) was washed with aqueous sodium hydroxide solution and water before drying over anhydrous magnesium sulfate and distilling under reduced pressure.

MMA and MPEG were simultaneously dissolved in ethanol (200 mL/mol of monomers) together with azo bis(isobutyronitrile) (AIBN) such that the mole ratio of AIBN to all monomer species was 1:220. This solution was placed in a dropping funnel fitted to a flask containing ethanol (10 mL). The flask

Table 1. Composition, Molar Mass, and Polydispersity Indices for Copolymers

copolymer	MPEG:MMA	weight fraction of EO	$10^3\bar{M}_w$	$\bar{M}_w/\bar{M}_n$
60CP	1:56 ± 2	0.30 ± 0.01	83.6	1.5
D60CP	1:59 ± 3	0.29 ± 0.1	56.8	2.4
20CP	1:19 ± 2	0.55 ± 0.03	96.9	1.6
D20CP	1:16 ± 3	0.60 ± 0.04	71.1	1.7
10CP	1:12 ± 2	0.70 ± 0.04	120.4	1.4
D10CP	1:11 ± 1	0.66 ± 0.02	82.7	2.1

was fitted with a condenser and the contents of the flask were quickly brought to reflux while the whole apparatus was purged continuously with nitrogen. The monomer plus AIBN solution was then added dropwise over 1 h and the resulting viscous solution refluxed for a further hour, after which it was poured into chilled hexane. The resultant tacky precipitate was dried under vacuum at ambient temperatures. The general formula for the copolymer is and the purification

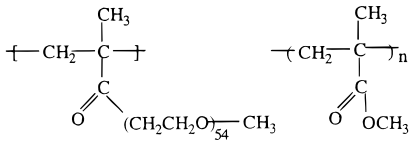

procedure depended on the value of *n*. Three copolymers were prepared with values of *n* of 60, 20, and 10; we refer to each of these copolymers as 60CP, 20CP, and 10CP.

None of the copolymers was water soluble and thus residual MPEG monomer was removed from 60CP and 20CP by stirring each copolymer in excess water followed by filtration, washing, and drying under vacuum. This procedure could not be used for 10CP since the copolymer became highly swollen and gellike. The procedure adopted was to dissolve the copolymer in ethanol and then to precipitate it fractionally by addition of hexane. The polymer rich phase that settled out was drawn off and poured into chilled hexane. A white powder resulted, which was filtered off and dried under vacuum.

The same synthesis and purification procedures were applied to copolymers prepared using perdeuteriomethyl methacrylate. All copolymers were analyzed using both ^{1}H NMR and elemental analysis and these compositions are reported as a mole ratio and as a percentage by mass of ethylene oxide in Table 1. Molar masses were obtained by size exclusion chromatography on chloroform solutions using polystyrene standards as calibrants; these values are also reported in Table 1.

Surface Pressure Isotherms. Surface pressure isotherms for each copolymer were obtained using a NIMA (Coventry, U.K.) Langmuir trough, model 200l. Each copolymer was spread onto freshly aspirated and cleaned pure water (electrochemical grade) by deposition from chloroform solution. The spread films, covering an area of 900 cm^2, were compressed at 30 cm^2 min^{-1} and the surface pressures recorded continuously. Figure 1 shows the surface pressure isotherms recorded for each copolymer at 296 K. Deuteration of polymers (and their solvents) frequently leads to observable effects on thermodynamic properties, especially in the vicinity of phase transitions; however, no effect of deuteration on the surface pressure isotherms was noted. Figure 1 shows distinctive changes in surface pressure for relatively modest changes in ethylene oxide content. All the isotherms exhibit characteristics of spread films of both homopolymers. Finite values of the surface pressure are noted at low surface concentrations and the surface pressure increases smoothly. This is very similar to that for spread PEO films. However, the plateau surface pressure of 10 mN m^{-1} observed for PEO is not observed for the graft copolymers. A pseudoplateau is seen in all copolymers, the extent of which decreases as the PEO content of the copolymers increases. The surface pressure then increases to higher values in a manner akin to that of spread films of poly(methyl methacrylate); over the range of surface concentration (Γ_s) explored here, we do not observe the plateau

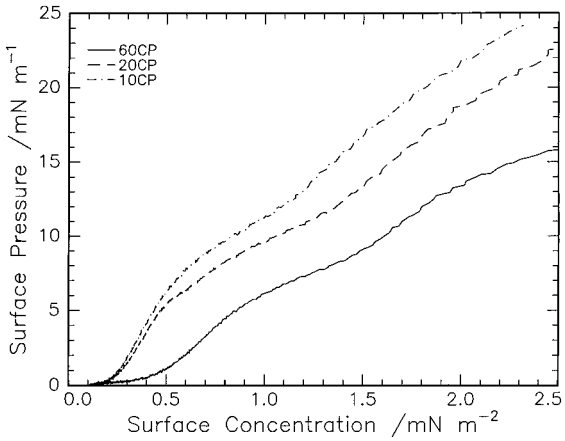

Figure 1. Surface pressure as a function of surface concentration for each graft copolymer at 298 K.

surface pressure of PMMA, which is ca. 30 mN m^{-1}. Repeated determination of surface pressure isotherms for the same copolymer were essentially indistinguishable from each other.

Neutron Reflectometry. Neutron reflectometry data were obtained using the CRISP reflectometer located on the U.K. pulsed neutron source, ISIS, at the Rutherford-Appleton Laboratory, Didcot, Oxfordshire. The incident neutron wavelength range was from 0.5 to 6.5 Å, and two grazing incidence angles were used, 0.8° and 1.5°. This provided an accessible range of momentum transfer, Q, of $0.02 \leq Q/\text{Å}^{-1} \leq 0.65$. A rectangular NIMA trough was mounted in the path of the incident beam on a vibration damping plinth and enclosed in a sealed box to prevent excessive evaporative exchange between the aqueous subphase and the surrounding atmosphere. The neutron beam entered and exited the box via quartz windows; beam height was defined by a slit immediately before the entrance window. The resolution in Q was constant at 4% over all the Q range, the detector was a single time-of-flight, He-filled detector, and the incident beam was monitored by a similar but lower efficiency detector through which the incident beam passed. All neutron reflectometry data were placed on an absolute scale by calibration of the instrument using clean D_2O. Two aqueous subphases were used; D_2O and that mixture of D_2O and H_2O which has a net scattering length density of zero and which will be referred to as null reflecting water (NRW). The combinations of copolymer and subphases used in the reflectometry experiments were chosen to maximize the information obtainable. Consequently, the combinations used were hydrogenous copolymers on D_2O and part deuterated copolymers on NRW and D_2O.

Results

Details of the analysis methods are set out below for the 20CP graft copolymer; the same procedures were used for the 10CP and 60CP graft copolymers.

20CP Graft Copolymers. Figure 2 shows reflectivities obtained for the D20CP on null reflecting water. The source of the reflectivity is the deuteriopoly(methyl methacrylate) backbone, and the increasing reflectivity with surface composition indicates that the composition of the backbone-containing layer changes with increasing Γ_s. From these data alone it is impossible to tell whether the backbone layer is diluted by both subphase and EO or just one of them. Notwithstanding the change in absolute reflectivities, the shapes of the curves are similar (in particular at low Q the reflectivity curves are essentially identically steep), indicating that this backbone-containing layer does not change its dimensions significantly when Γ_s is increased. At first glance, the reflectivities of the D20CP when spread on D_2O

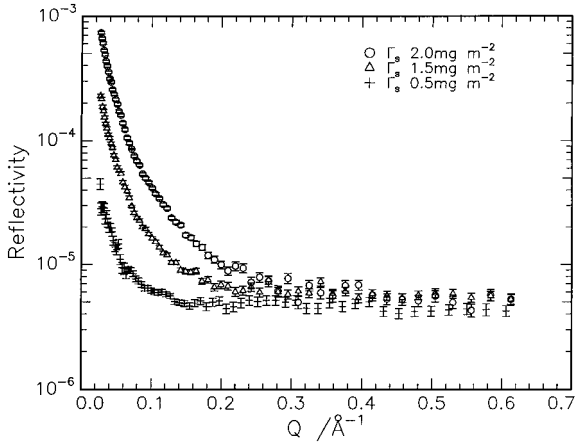

Figure 2. Reflectivity data for D20CP graft copolymer spread on null reflecting water at the surface concentrations indicated.

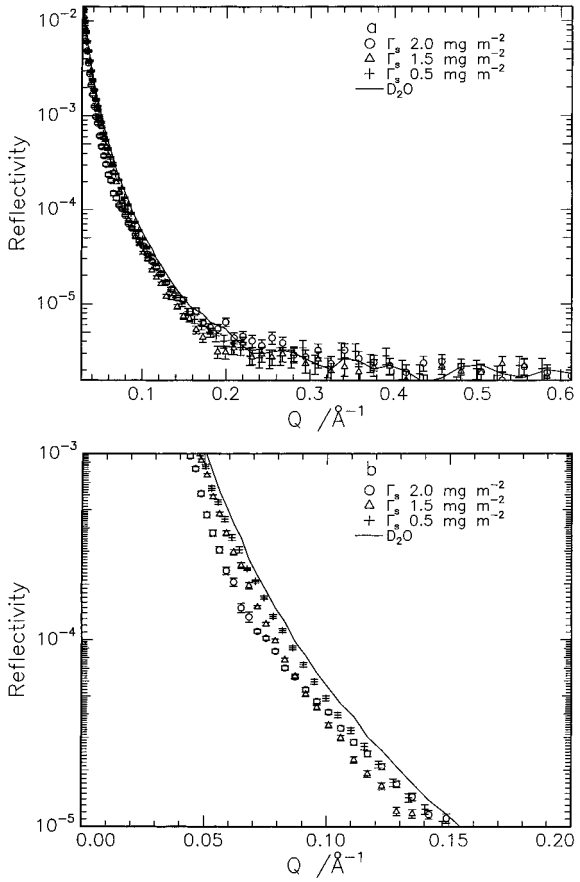

Figure 3. (a) Reflectivity data for D20CP graft copolymer spread on D_2O at the three surface concentrations investigated. The solid line is the reflectivity of D_2O under the same conditions. (b) Enlargement of part of Figure 3a showing the differences in reflectivities.

(Figure 3a) appear to be identical. Careful inspection reveals subtle differences between the reflectivity when $\Gamma_s = 2.0$ mg m^{-2} and the reflectivities at the two lower surface concentrations. At the two lower surface concentrations the reflectivities are essentially identical in shape; however, the reflectivity curve for the highest Γ_s crosses these two reflectivity profiles and has a distinctly different shape (Figure 3b). It is the hydrogenous poly(ethylene oxide) grafts that influence the reflectivity in this combination, and there is a change in the organization of the EO-containing layers at the highest surface concentration.

Reflectometry data were analyzed using the exact optical matrix method. For each surface concentration of copolymer, a model of the copolymer organization was adopted and the parameters (thickness and scattering length density of each layer) adjusted to give the best nonlinear least-squares fit to the reflectivity data for one set of contrast conditions. These parameters were then applied to the other contrast conditions used at the same surface concentration and the process iterated until the same model fitted all contrast conditions. A further check was the calculation of the surface concentration of copolymer (either in toto or separately for each constituent) and comparison with the amount dispensed onto the surface.

The models used were a series of uniform layers, the parameters of which are the scattering length density, ρ, and layer thickness, d, both of which are the adjustable variables in fitting the experimental reflectivity profiles. With these parameters at hand other characteristic factors for each layer can be calculated, thus,

$$\rho = \sum \rho_i \phi_i \tag{5}$$

Where ρ_i and ϕ_i are the scattering length densities and volume fraction of each species i in the layer. Knowing the coherent scattering length, b_i, of this same species then its number density is obtainable from

$$n_i = \phi_i \rho_i / b_i \tag{6}$$

and the surface concentration of the species in generally accepted units is

$$\Gamma_s = \frac{n_i m_i d}{N_A} \times 10^{20} \text{ mg m}^{-2} \tag{7}$$

with m_i the molecular weight of species i and N_A Avogadro's number.

In attempting to arrive at a model for the organization of the graft copolymer at the air−water interface, we started with the simplest possible model and introduced additional features where no satisfactory agreement with the experimental data could be obtained. Initially, a single uniform layer model was adopted; additional layers were incorporated (i.e., two or three layer models) as necessary to provide the best fit to the reflectivity profiles obtained at all contrast conditions. The absence of graft copolymers with deuterated ethylene oxide grafts is a disadvantage since the influence of the grafts on the reflectivity will be a "second-order" effect. By this we mean that because the scattering length density of hydrogenous ethylene oxide is low (0.57×10^{-6} Å^{-2}), the presence of the grafts when the graft copolymer is spread on D_2O will be signaled by the reduction in the reflectivity relative to that of clean D_2O.

Summarizing the results of this optical matrix analysis, at the lowest surface concentration of graft copolymer a single layer of MMA was sufficient but two layers of EO were needed to reproduce the reflectivity. At higher surface concentrations, two layers of MMA were required and eventually a three-layer model for the distribution of EO was necessary at the highest surface concentration. Figure 4 shows the fit of a three-layer model for D20CP spread on D_2O at 2.0 mg m^{-2}.

The scattering length density of any layer i is given by $\rho_i = \phi_m \rho_m + \phi_e \rho_e + (1 - \phi_e - \phi_m)\rho_s$ and for each layer we can write two such equations, one pertaining to

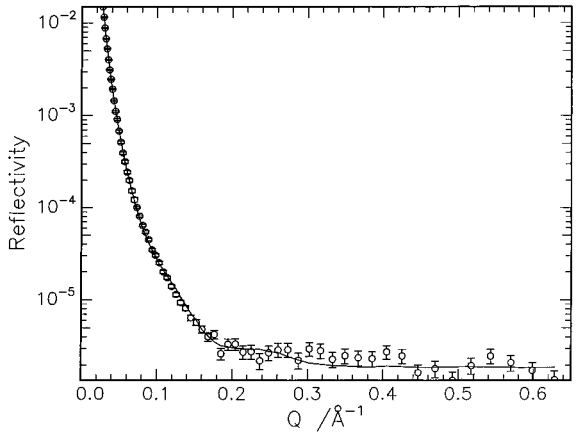

Figure 4. Three-layer model fit of the reflectivity from D20CP spread on D_2O at 2.0 mg m^{-2}.

Table 2. Volume Fraction Compositions and Layer Thicknesses from Reflectivity Data

copolymer	Γ_s/mg m^{-2}	layer	d/Å	ϕ_{MMA}	ϕ_{EO}	ϕ_w
10CP	0.4	1	16 + 1	0.02	0.13	0.86
		2	49 + 2	0.01	0.03	0.94
10CP	1.1	1	12 + 2	0.13	0.38	0.49
		2	24 + 4	0.05	0.08	0.87
		3	45 + 3	0	0.02	0.9
20CP	0.5	1	10 + 1	0.08	0.07	0.85
		2	20 + 1	0	0.07	0.93
20CP	1.5	1	12 + 1	0.42	0.24	0.34
		2	28 + 1	0.02	0.07	0.91
20CP	2.0	1	10 + 2	0.9	0	0
		2	23 + 1	0.06	0.2	0.74
		3	24 + 2	0	0.11	0.89
60CP	1.6	1	9 + 1	0.75	0	0
		2	8 + 1	0.69	0.08	0.23
		3	30 + 2	0	0.06	0.94

D20CP spread on D_2O and the other for 20CP on D_2O. These two equations were solved simultaneously for the volume fractions composition of each layer (because the scattering length densities are known) given in Table 2. The volume fraction of MMA obtained in this way for layer 1 (the uppermost layer) was in good agreement with that obtained from the reflectivity of D20CP on NRW where only the DMMA contributes to the reflectivity. The results of this analysis are combined with layer thickness, and the volume fraction profiles in Figure 5 represent the organization of the graft copolymer that reproduces the reflectivity profiles.

10CP and 60CP Graft Copolymers. Only two concentrations of the 10CP and 60CP copolymers (and their part deuterated versions) have been investigated by neutron reflectometry, and these data were analyzed in the same way as for 20CP. For 10CP a two-layer model reproduced the reflectivity data well for the lowest surface concentration of 0.4 mg m^{-2}. At 1.1 mg m^{-2}, a three-layer model was required to obtain an acceptable fit to the data. Similarly, for the 60CP, at the lowest surface concentration (0.65 mg m^{-2}) a two-layer model reproduces the reflectivities under all contrast conditions whereas at the higher surface concentration of 1.6 mg m^{-2} a three-layer model provides a good description of the reflectivity data. The thickness and volume fraction of the layers for each of these graft copolymers are given in Table 2.

Discussion

The surface concentration of each copolymer in mg m^{-2} has been calculated from the volume fraction and thickness of each layer, and Table 3 gives the comparison to the amounts spread. Table 3 shows the average weight fraction composition of the copolymer obtained from the surface concentrations of the MMA and EO components determined from the neutron reflectometry data. For the 10CP copolymer the calculated surface concentration is in good agreement with the spread amount, the calculated weight fraction of ethylene oxide in the copolymer is in reasonable agreement with analytical data. For 20CP the agreement between surface concentrations and graft copolymer compositions calculated from neutron reflectometry data and the

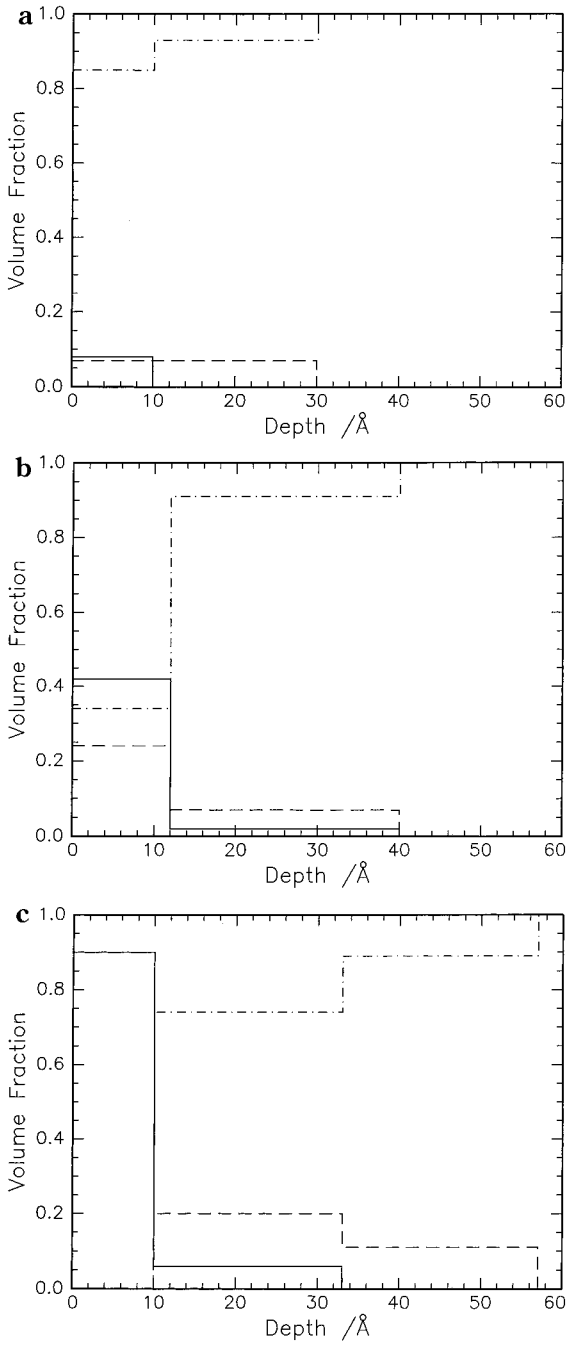

Figure 5. Volume fraction of the components as a function of depth below surface for the 20CP graft copolymer spread on water, as obtained from simple layer model fits to neutron reflectivity data for the three surface concentrations investigated: (a) Γ_s = 0.5 mg m^{-2}; (b) Γ_s = 1.5 mg m^{-2}; (c) Γ_s = 2.0 mg m^{-2}. For each concentration the individual components are indicated by (—) MMA; (···) EO; (—·—) Water

Table 3. Calculated Surface Concentrations, Γ_s^c, from Fits to Neutron Reflectivity Data Using Exact Optical Matrix Calculation

copolymer	Γ_s/mg m^{-2}	Γ_s^c, /mg m^{-2}	w^c_{EO}
10CP	0.4	0.44	0.75
	1.1	1.04	
	0.5	0.30	
20CP	1.5	1.10	0.52
	2.0	1.80	
60CP	0.65	0.54	0.27
	1.6	1.58	

actual values is slightly poorer. In particular, we note that the calculated weight fraction of EO is lower than that obtained by analysis. This may be due to the high dilution of the EO and the resultant small contribution to the reflectivity being overwhelmed by that of the MMA backbone. Consequently, analysis of the reflectivity fails to account for all of the EO present. This view is also consistent with the results obtained from analysis of the reflectivity of spread 60CP layers. In all cases the calculated values of Γ_s are slightly smaller than that actually spread.

To make some general conclusions about the organization of the copolymer at the air−water interface, we must compare those surface concentrations where the total EO concentration is similar, i.e., 10CP at $\Gamma_s = 0.4$ mg m^{-2}, 20CP at $\Gamma_s = 0.5$ mg m^{-2}, and 60CP at $\Gamma_s = 0.65$ mg m^{-2}. As the MMA content of the copolymer increases, so does that of the upper layer, the layer becomes thinner, and for the 60CP copolymer the layer thickness is just larger than the diameter of the poly(methyl methacrylate) molecules. For each copolymer at its selected concentration, two layers are required to describe the interface observed; in all cases the second lower layer is thick, particularly so for 10CP material, indicating that the EO grafts penetrate the subphase to a significant depth. For 10CP, this second layer also contains a small amount of MMA, probably those segments bearing the EO grafts, which being more numerous make a greater contribution to the reflectivity than in the 20CP and 60CP copolymers. The general conclusion is that, for equal amounts of EO at the interface between air and water, increasing the MMA content leads to considerable enrichment of the MMA in the upper layer, forming a layer thinner than has been observed for spread films of poly(methyl methacrylate) homopolymer.

A similar comparison can also be made between 10CP at 1.1 mg m^{-2} and 20CP at 1.5 mg m^{-2}, the surface concentration of EO in each case being 0.8 ± 0.1 mg m^{-2}; the increased graft frequency in 10CP makes the grafts explore greater subphase depths. This suggests a more general way of analyzing the data, i.e., via the "grafting" density or number of EO grafts per unit interface area, σ, of the interface. To calculate σ, we make two assumptions: (i) all the EO grafts penetrate the subphase, and (ii) the EO grafts are equally spaced along the MMA backbone. We accept that these assumptions may not be wholly true and the values of σ incorrect in absolute terms, but for a relative comparison of the spread graft copolymer film with each other they will be valid. The dependence of brush height or thickness, h, on σ is given by[12,13]

$$h \propto \sigma^{1/3} \tag{8}$$

The total thickness of the EO-containing layers obtained had a scattered linear dependence on σ, and the exponent cannot be evaluated with confidence.

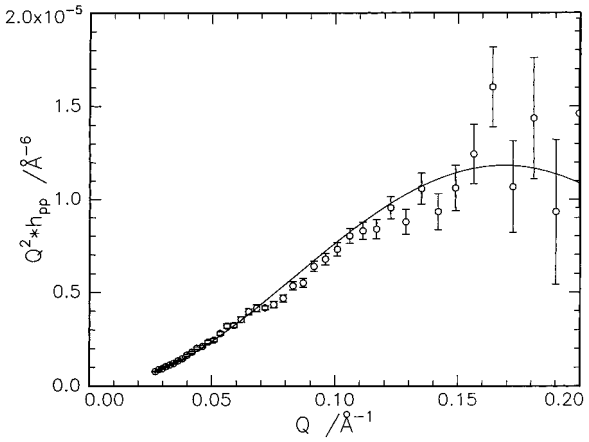

Figure 6. Uniform layer partial structure factor (solid line) fitted to neutron reflectivity data (plotted in the kinematic approximation form) for D20CP copolymer spread on NRW at 1.5 mg m^{-2}.

A complete description of the surface organization, in principle, is obtainable by analysis of the reflectivity data using the kinematic approximation. However, this requires that each component of the copolymer be deuterium labeled, and this option was not available. A partial analysis of the neutron reflectometry data using the kinematic approximation was made by making approximations based on the magnitude of the scattering length densities. Thus, when the deutero graft copolymers are spread on NRW, we can approximate the scattering length density of the hydrogenous EO grafts to zero and hence eq 4 becomes

$$R(Q) = \frac{16\pi^2}{Q^2} b_m{}^2 h_{mm}(Q) \tag{9}$$

In a like manner, when the totally hydrogenous copolymer is spread on D_2O, we approximate the scattering length density of the copolymer to zero and the specular reflectivity is given by

$$R(Q) = \frac{16\pi^2}{Q^2} b_s{}^2 h_{ss}(Q) \tag{10}$$

Note that both eqs 9 and 10 pertain to background-subtracted reflectivity data.

The partial structure factor for a uniform layer[33] was fitted to h_{mm} (Q) obtained from the reflectivity (via eq 9) with the number density of MMA segments, n_m, and layer of thickness d_m as fitting variables; a typical fit is shown in Figure 6. The near surface water layer was also modeled as a uniform layer,[33] and the number density and thickness of this water layer were also obtained by fitting.

The number density and layer thickness obtained using these approximate partial structure factors are given in Table 4, which also contains the total surface concentration of copolymer calculated from n_m and the known composition of the copolymer. For the 60CP copolymer the thicknesses of MMA-containing layers are in very good agreement with those obtained using the exact optical matrix analysis. (Partial structure factor analysis gives the *total* thickness of the MMA-containing layer; e.g., for $\Gamma_s = 1.6$ mg m^{-2}, the thickness is equivalent to layers 1 and 2 in the optical matrix results

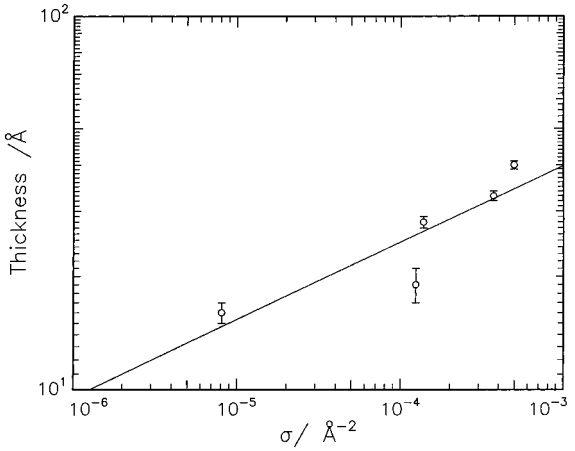

Figure 7. Double logarithmic plot of the near surface water layer as a function of the grafting density. The solid line is a linear least-squares fit to the data.

Table 4. Number Densities and Layer Thicknesses from Partial Structure Factors

copolymer	Γ_s/mg m^{-2}	$n_m/10^{-2}$ Å^{-3}	d_m/Å	Γ_s^c/mg m^{-2}	$n_s/10^{-2}$ Å^{-3}	d_s/Å
20CP	0.5				0.31 + 0.03	19
	1.5	0.18 + 0.01	18 + 1	0.97 + 0.03	0.48 + 0.02	33
	2.0	0.37 + 0.01	15 + 1	1.54 + 0.3	0.67 + 0.02	40
60CP	0.65	0.19 + 0.01	10 + 1	0.45	0.37 + 0.03	16
	1.60	0.41 + 0.01	17 + 1	1.65 + 0.15	0.46 + 0.01	28
10CP	1.1	0.16 + 0.01	14 + 1	0.4 + 1		

of Table 2.) The surface concentrations calculated from the parameters of this kinematic approximation analysis are in reasonable agreement with the amounts spread. For the 20CP copolymer the MMA layer thickness is closer to the layer 1 thickness in Table 2, since this contains the majority of the MMA. This failure to account properly for all of the MMA segments is reflected in the low values of total surface concentration calculated from n_m relative to the actual amount of copolymer spread on the aqueous subphase.

The water layer thickness obtained correlates qualitatively with the lower layer thickness (layer 2 or layers 2 and 3 in Table 2) obtained by the optical matrix analysis, and as Γ_s increases so does the value of d_s. If the near surface water layer is associated with the EO segments, then the increased thickness is due to the EO layer extending deeper into the subphase as the effective grafting density increases. Figure 7 is a double-logarithmic plot of d_s as a function of σ, and a linear least-squares fit to these data gives a scaling relation of

$$\text{thickness} \propto \sigma^{0.21}$$

The exponent is significantly smaller than the value of 0.3 predicted theoretically for a stretched wet brush. The EO grafts appear to fulfill all the conditions of a wet brush; there is evidently considerable penetration of the brush layer by the solvent; and the aqueous subphase is a thermodynamically good solvent for the grafts, and hence we anticipate the grafts to be swollen to their excluded volume limit. However, the grafts have only a limited number of segments and the excluded volume swelling may be small and the entropic penalty in adopting a stretched configuration sufficiently large to prevent full stretching. The radius of gyration of the grafts would be expected to be ca. 25−30 Å if dilute solution data for PEO are applicable to the low molecular weights of the grafts. The ratio of the EO-containing layer thickness to this radius of gyration ranges from 1 (for 60CP) to ca. 3 for 10CP. These values are significantly smaller than the value of 5 accepted as typical for a stretched wet brush layer. An additional factor is the surface tension of the polymer film covered water. Even at the highest concentration of graft copolymer, the surface tension is ca. 60 mN m^{-1}, which is approximately double the surface tension of a melt of poly(ethylene oxide). Consequently, the EO segments will preferentially populate the air−water interface to reduce the surface energy. Only when the surface tension is reduced to that of PEO will this resistance to chain extension be removed.

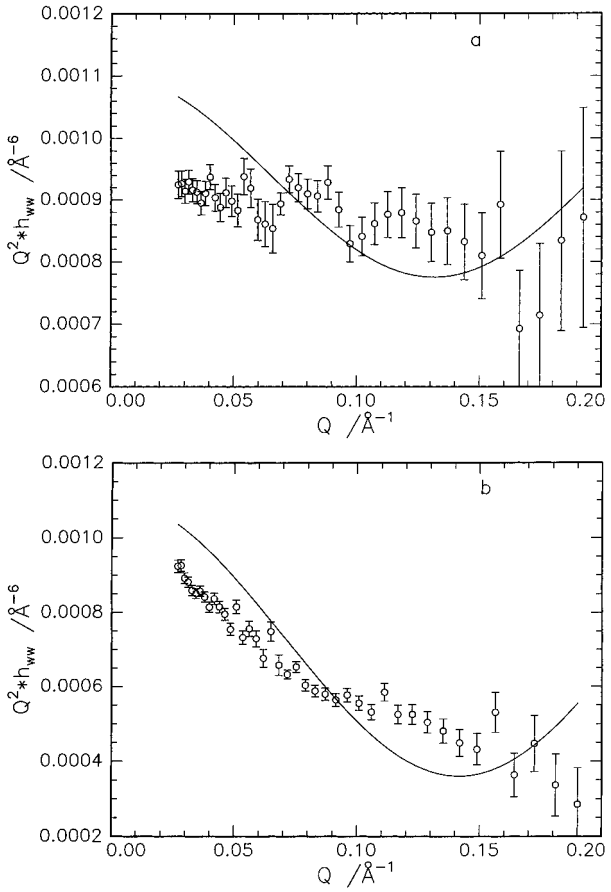

Figure 8. Neutron reflectivity data for 10CP spread on D_2O plotted in the kinematic approximation form for the two surface concentrations of (a) 0.4 mg m^{-2} and (b) 1.1 mg m^{-2}.

At this juncture it is appropriate to make some remarks concerning the partial structure factors for water for the 10CP copolymer. These are reproduced in Figure 8. At low values of Q, they have a character different from those of 20CP and 60CP and could not by any means be smoothly extrapolated to the $Q = 0$ value for water of $m_s^{\infty 2}$ of 1.1×10^{-3} Å^{-6}. Such behavior is also evident in the water partial structure factor for the surface excess layer in poly(ethylene oxide) solutions and is also evident in those for the nonionic surfactants of the C_nE_m variety. The common factor to all of these situations is the relatively high concentration of EO segments at the air−water interface. Clearly, the partial structure factor has to produce the correct value of the number density of water in the bulk, and therefore, it appears that an additional term (or terms) must be added to eq 12 to account for the features between $Q = 0$ and the value of Q where the partial

structure factor can be described by eq 12. Although it is known that poly(ethylene oxide) structures water around itself, it is difficult to see how a polymer that is essentially confined to within 50 Å of the surface can produce a structural effect in the subphase at distances of ca. 300 Å ($\sim 2\pi/Q_{min}$). To evaluate this behavior in detail requires reflectivity data at much lower Q values than those currently accessible, and these data can only be obtained using NRW as the subphase because critical reflection intervenes at $Q \sim 0.018$ Å^{-1} for D_2O subphases. Without such data the source of this behavior will remain unclear; it is, however a real effect that is common in ethylene oxide containing systems.

Conclusions

Graft copolymers consisting of a poly(methyl methacrylate) backbone with poly(ethylene oxide) are able to be spread at the air−water interface. The copolymer arrangement is determined by the surface concentration and the copolymer composition, and as the surface concentration increases, the number of layers needed to describe the organization of the spread film increases. With increasing poly(ethylene oxide) content of the graft copolymers, the surface concentration at which more than two layers are needed to reproduce the reflectivity data decreases, with the deeper layers containing poly(ethylene oxide) and water only. From the dependence of layer numbers and layer thickness on concentration and composition, we conclude that it is the areal density of poly(ethylene oxide) grafts that is the major controlling factor. The solvated grafts have been likened to the much discussed polymer brushes, and the thickness of the poly(ethylene oxide) layers displays a dependence on the grafting density that is smaller than that predicted by either scaling or exact theories of the grafted brush. The low molecular weight of the grafts and the high surface tension of water have been cited as the reasons for incomplete agreement with theoretical predictions. When the concentration of poly(ethylene oxide) grafts in the near surface water layer is high, the partial structure factor for the water layer displays anomalous behavior at low Q values (i.e., deep in the subphase). The reasons for such behavior are not clear, but it is a general observation for all systems (nonpolymeric as well as polymeric) where the ethylene oxide content is high.

Acknowledgment. R.W.R. thanks the EPSRC for support of the research program of which this work is a part. S.K.P. thanks EPSRC and ICI Paints for a CASE maintenance award. Both R.W.R. and S.K.P. are grateful to CLRC and in particular ISIS for the provision of neutron beams and instrumentation.

References and Notes

(1) Earnshaw, J. C. In *Light Scattering at the Fluid Interface*; Earnshaw, J. C., Ed.; Wiley: New York, 1986.
(2) Earnshaw, J. C.; McGivern, R. C. *J. Phy. D: Appl. Phys.* **1987**, *20*, 82.
(3) Langevin, D. *Light Scattering by Liquid Surfaces and Complementary Techniques*; Marcel Dekker: New York, 1992; Vol. 41.
(4) Levich, V. G. *Physicochemical Hydrodynamics*; Prentice-Hall: Englewood Cliffs, NJ, 1962.
(5) Mann, E. K.; Lee, L. T.; Henon, S.; Langevin, D.; Meunier, J. *Macromolecules* **1993**, *26*, 7307.
(6) Amile, C.; Sikka, M.; Schneider, J. W.; Tsao, Y. H.; Tirrel, M.; Mays, J. W. *Macromolecules* **1995**, *25*, 3125.
(7) Sauer, B. B.; Yu, H.; Yazdanian, M.; Zografi, G.; Kim, M. W. *Macromolecules* **1989**, *22*, 2232.
(8) Brinkhuis, R. H. G.; Schouten, A. J. *Macromolecules* **1991**, *24*, 1487.
(9) Brinkhuis, R. H. G.; Schouten, A. J. *Macromolecules* **1992**, *25*, 2725.
(10) Styrkas, D. A.; Thomas, R. K.; Adib, Z. A.; Davis, F.; Hodge, P.; Liu, X. H. *Macromolecules* **1994**, *27*, 5504.
(11) Styrkas, D. A.; Thomas, R. K.; Sukhorukov, A. V. *Thin Solid Films* **1994**, *243*, 437.
(12) de Gennes, P. G. *Macromolecules* **1980**, *13*, 1069.
(13) Milner, S. T.; Witten, T. A.; Cates, M. E. *Macromolecules* **1988**, *21*, 2610.
(14) Milner, S. T.; Witten, T. A.; Cates, M. E. *Macromolecules* **1989**, *22*, 853.
(15) Auroy, P.; Auvray, L.; Leger, L. *Macromolecules* **1991**, *24*, 2523.
(16) Cosgrove, T.; Heath, T.; Vanlent, B.; Leermakers, F.; Scheutjens, J. *Macromolecules* **1987**, *20*, 1692.
(17) Cosgrove, T.; Heath, T. G.; Ryan, K.; Vanlent, B. *Polym. Commun.* **1987**, *28*, 64.
(18) Klein, J.; Luckham, P. F. *Macromolecules* **1984**, *17*, 1041.
(19) Luckham, P. F.; Klein, J. *J. Chem. Soc., Faraday Trans. 1* **1990**, *86*, 1363.
(20) Patel, S.; Tirrell, M.; Hadziioannou, G. *Colloids Surf.* **1988**, *31*, 157.
(21) Patel, S.; Tirrell, M. *Annu. Rev. Phys. Chem.* **1989**, *40*, 597.
(22) Watanabe, H.; Tirrell, M. *Macromolecules* **1993**, *26*, 6455.
(23) Clarke, C. J.; Jones, R. A. L.; Edwards, J. L.; Clough, A. S.; Penfold, J. *Polymer* **1994**, *35*, 4065.
(24) Clarke, C. J.; Jones, R. A. L.; Edwards, J. L.; Shull, K. R.; Penfold, J. *Macromolecules* **1995**, *28*, 2042.
(25) Hopkinson, I.; Kiff, F. T.; Richards, R. W.; Bucknall, D. G.; Clough, A. S. *Polymer* **1997**, *38*, 87.
(26) Kent, M. S.; Lee, L.-T.; Factor, B. J.; Rondelez, B. J.; Smith, G. S. *J. Chem. Phys.* **1995**, *103*, 2320.
(27) Field, J. B.; Toprakcioglu, C.; Ball, R. C.; Stanley, H. B.; Dai, L.; Barford, W.; Penfold, J.; Smith, G.; Hamilton, W. *Macromolecules* **1992**, *25*, 434.
(28) Lu, J. R.; Su, T. J.; Thomas, R. K.; Penfold, J.; Richards, R. W. *Polymer* **1996**, *37*, 109.
(29) Henderson, J. A.; Richards, R. W.; Penfold, J.; Thomas, R. K.; Lu, J. R. *Macromolecules* **1993**, *26*, 4591.
(30) Richards, R. W.; Rochford, B. R.; Webster, J. R. P. *Faraday Discuss.* **1994**, *98*, 263.
(31) Richards, R. W.; Rochford, B. R.; Taylor, M. R. *Macromolecules* **1996**, *29*, 1980.
(32) Lekner, J. *Theory of Reflection*; Martinus Nijhoff: Dordrecht, The Netherlands, 1987.
(33) Thomas, R. K. *Neutron Reflection from Polymer Bearing Surfaces*; Richards, R. W., Ed.; Ellis Horwood: London, 1995.
(34) Russell, T. P. *Materials Science Reports* **1990**, *5*, 171.

MA970363S